Dielectric tube Terahertz waveguide with anti-reflection structure

Dominik Walter Vogt and Rainer Leonhardt
Dodd-Walls Centre for Photonic and Quantum Technologies,
Department of Physics, The University of Auckland, Private Bag 92019, Auckland, New Zealand
Email: d.vogt@auckland.ac.nz

***Abstract*—We numerically study the guidance properties of a dielectric tube Terahertz (THz) waveguide with an anti-reflection (AR) structure to efficiently extend the bandwidth of a low loss dielectric tube waveguide. The results obtained from the 3D finite-difference time-domain (FDTD) simulations are in excellent agreement with THz time-domain spectroscopy (THz-TDS) measurements of 3D-printed prototypes of the novel THz waveguides. The presented AR-structure consists of dielectric close-packed cones arranged in a hexagonal lattice on the outer circumference of the dielectric tube. With feature sizes of about 600 μm and 1200 μm the investigated cones are in the order of the wavelength between 0.2 THz to 1 THz.**

I. Introduction

Waveguides for the unique THz frequency range (0.1 THz to 10 THz) [1] are very challenging to realize due to a lack of suitable materials [2]. A promising candidate for low loss and low dispersion guidance of THz radiation is a plain dielectric tube [3]. The cladding of the tube acts as a Fabry-Perot etalon and thus confines the guided Terahertz radiation in the core of the waveguide. This hollow core principle overcomes high waveguide losses caused by material absorption. However, the attenuation spectrum of the dielectric tube resembles the typical transmission function of a Fabry-Perot etalon, and therefore limiting the bandwidth of the waveguide.

We propose a dielectric tube THz waveguide with an anti-reflection structure to suppress the interference in the waveguide core originated by the Fabry-Perot effect of the tube cladding. The AR-tube waveguide provides a highly extended bandwidth compared to a plain dielectric tube while maintaining its low loss guidance.

II. Results

The numerical characterization of the AR-tube waveguides is performed with 3D FDTD simulations. The time-domain method is particularly suitable to study the broadband behavior of the waveguides. All simulations are implemented with the open source software MIT Electromagnetic Equation Propagation (MEEP) [4].

A cross section of a typical 3D computational cell is shown in Fig. 1 (a) along with a picture of the close-packed hexagonal lattice AR-structure in Fig. 1 (b). The AR-tube waveguides studied in this work have an inner diameter of 4 mm and a cladding thickness of 600 μm. The effect of the AR-structure is investigated with both 14 and 28 close-packed cones along

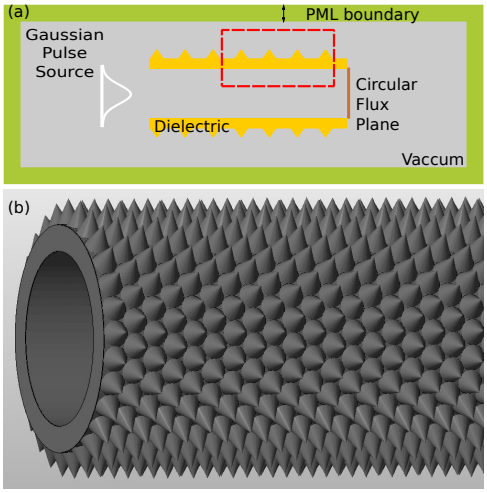

Fig. 1. (a) Cross section of a schematic model of the 3D computational cell used in the FDTD simulations. The red rectangular indicates the area where the fields shown in Fig. 2 are extracted. A mesh size of 25 μm was chosen to ensure a sufficient resolution for the frequency range from 0.2 THz to 1 THz and (b) CAD model of the 28 cones AR-tube waveguide. The cones are arranged in a close-packed hexagonal lattice.

the outer circumference of the tube waveguide. With heights of about 600 μm (28 cones) and 1200 μm (14 cones) and an apex angle of 50 degrees, the cones are about one and two wavelengths at 0.5 THz, respectively.

The complex refractive index of the waveguide dielectric material is modeled with a Lorentzian susceptibility, based on the experimentally determined parameters of the 3D-printing material (see [5]).

A linear-polarized ultrashort Gaussian pulse current source (bandwidth: 0.1 THz to 1.1 THz) at the input end of the waveguide excites the modes propagating in the waveguide. Figs. 2 (a) - (c) show the guided electric field energy density distributions in vicinity of the waveguide cladding for a dielectric tube, 14 cones AR-tube and 28 cones AR-tube, respectively, on a logarithmic scale at the same instant. Fig. 2 (a) clearly shows the Fabry-Perot effect of the tube cladding and the afterpulses propagating in the waveguide core originated from the reflections on the outer surface of the tube cladding. The AR-structure efficiently suppresses the reflections and the accompanying afterpulses,

978-1-4673-8603-6/16/$31.00 ©2016 IEEE

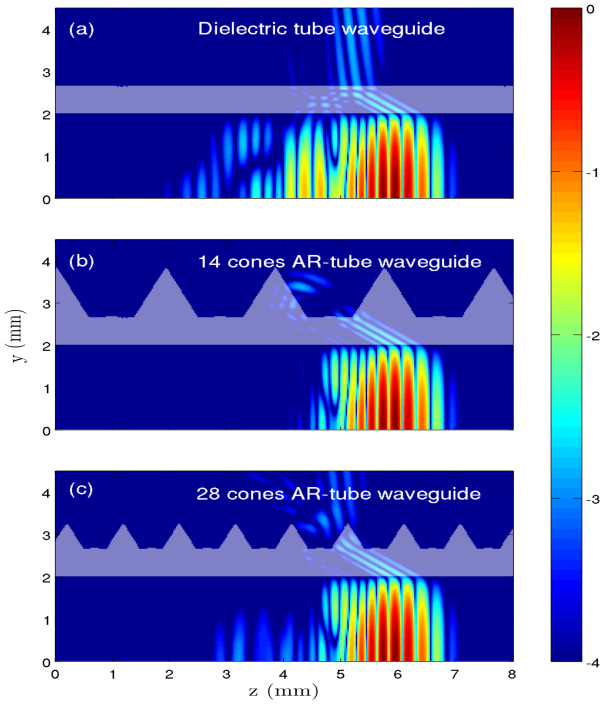

Fig. 2. Normalized spatial distribution of the simulated electric field energy density in the vicinity of the cladding of (a) a plain dielectric tube, (b) for a 14 cones AR-tube waveguide and (c) for a 28 cones AR-tube waveguide. The density distributions are shown on a logarithmic scale at the same instant. The THz pulse is propagating in the positive z-direction. The origin of each sub-figure sits on the center axis of the waveguides as indicated with the red rectangle in Fig. 1 (a).

as can be seen in Figs. 2 (b)-(c) for both AR-tube waveguides.

The attenuation spectrum of a waveguide is extracted from the 3D FDTD simulations by comparison of two transmission spectra for different waveguide lengths. This method ensures the elimination of coupling losses otherwise contributing to the attenuation coefficient. The transmitted power spectrum of a waveguide is obtained by computing a surface integral of the Poynting vector over a circular plane located at the waveguide's output end [see Fig. 1 (a)].

The numerically obtained attenuation spectra for both the plain tube (red solid line) and the AR-tube waveguides (blue and green solid lines for the 14 and 28 cones AR-tube waveguides, respectively) are shown in Fig. 3 in the frequency range from 0.2 THz to 1 THz on a logarithmic scale. The attenuation curves clearly reveal the extended bandwidth of the AR-tube waveguides compared to a standard dielectric tube with the prominent Fabry-Perot interference pattern. Moreover, both AR-tube waveguides show an attenuation close to the theoretical limit given by the Fabry-Perot effect free infinite cladding tube waveguide (black solid line).

Fig. 3 also shows the experimentally obtained attenuation curves for the tube (red dots) and both AR-tube waveguides with 14 cones (blue dots) and 28 cones (green dots). The AR-tube waveguide prototypes have been fabricated with a commercially available Project 3500HD Plus 3D printer with

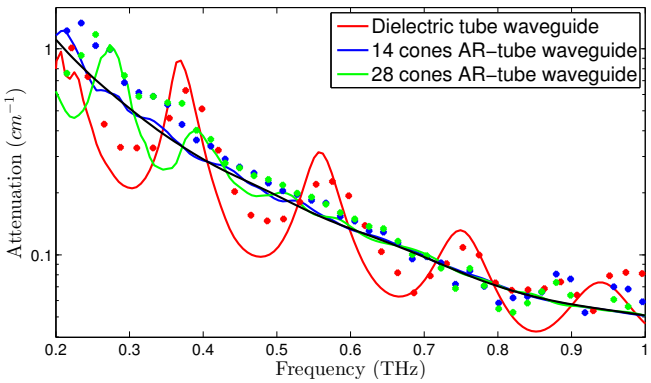

Fig. 3. Simulated (solid lines) and measured (dots) attenuation curves on logarithmic scale for a dielectric tube (red) and both AR-tube waveguides (14 and 28 cones in blue and green, respectively). The black solid line shows the theoretical attenuation limit of a Fabry-Perot effect free dielectric tube waveguide with an infinite cladding thickness.

a specified X-Y resolution of 375dpi (equivalent to 68 μm linewidth) and 790dpi in Z-resolution (equivalent to 32 μm linewidth) [6]. The THz-TDS measurements (for the THz-TDS setup description see [7]) agree very well with the 3D FDTD simulations over the entire frequency range from 0.2 THz to 1 THz, confirming the numerical results.

III. Conclusion

We observe broadband guidance of Terahertz radiation in a low loss dielectric tube waveguide with anti-reflection structure. The 3D FDTD simulations implemented with the open-source software MEEP to investigate the proposed AR-tube waveguides are presented. The electric field energy density distributions as well as the attenuation spectra extracted from the 3D FDTD simulations clearly reveal the superior guidance properties of the AR-tube waveguide. THz-TDS measurements of 3D-printed prototypes of the AR-tube waveguide confirm the 3D FDTD simulations as a powerful approach to study the AR-tube waveguides. Future work will focus on both numerical design optimization of the AR-structure and its experimental realization.

References

[1] M. Tonouchi, "Cutting-edge terahertz technology," *Nature Photonics*, vol. 1, no. 2, pp. 97–105, Feb. 2007.

[2] S. Atakaramians, S. Afshar V., T. M. Monro, and D. Abbott, "Terahertz dielectric waveguides," *Advances in Optics and Photonics*, vol. 5, no. 2, p. 169, Jun. 2013.

[3] H. Bao, K. Nielsen, O. Bang, and P. U. Jepsen, "Dielectric tube waveguides with absorptive cladding for broadband, low-dispersion and low loss THz guiding," *Scientific Reports*, vol. 5, p. 7620, Jan. 2015.

[4] A. F. Oskooi, D. Roundy, M. Ibanescu, P. Bermel, J. Joannopoulos, and S. G. Johnson, "Meep: A flexible free-software package for electromagnetic simulations by the FDTD method," *Computer Physics Communications*, vol. 181, no. 3, pp. 687–702, Mar. 2010.

[5] D. W. Vogt, J. Anthony, and R. Leonhardt, "Metallic and 3d-printed dielectric helical terahertz waveguides," *Optics Express*, vol. 23, no. 26, p. 33359, Dec. 2015.

[6] 3d systems. [Online]. Available: http://www.3dsystems.com

[7] J. Anthony, R. Leonhardt, and A. Argyros, "Hybrid hollow core fibers with embedded wires as THz waveguides," *Optics Express*, vol. 21, no. 3, p. 2903, Feb. 2013.